Estimation of the velocity at the impact of high rate sliding granular masses

Francesco Federico[1,*], and *Chiara* Cesali[1]

[1]University of Rome 'Tor Vergata', Department of Civil Engineering, Via del Politecnico 1, 00133 Rome, Italy

Abstract. Two analytical *block* models to estimate the maximum velocity reached by granular flows are proposed. The first one models the speed evolution of *coarse-grained* materials flows (e.g. debris flows, avalanches); it is based on the power balance of a granular mass sliding along planar surface, written by taking into account the volume of the debris mass, an assigned interstitial pressure, the energy dissipation due to *(i)* grain inelastic collisions ('granular temperature' within a basal '*shear layer*'); *(ii)* friction along sliding surface; *(iii)* fragmentation of grains. The second model allows to simulate the speed evolution of *fine-grained* materials flows (e.g. mudflows, quick clays) by taking into account the dissipation of the excess pore water pressure due to consolidation phenomena. Finally, the comparison between the results obtained through the proposed models and field and laboratory measures is carried out.

1 Introduction

Very high stresses arise at the contact surface between an impacting fluid and a solid body that constitutes an obstacle to the fluid flow; furthermore, these stresses act only for a very short time period. Thus, structures exposed to the impact with a fluid or a fluidized granular mass may be affected by serious damages, mainly due to the shock pressures. To avoid undesirable damages to inhabited areas, technical countermeasures (e.g. check dams, barriers and walls) must be put into action; their design must be based on the values of the impact force. Several relationships to estimate the maximum impact force per unit width (F) or pressure (p_{max}) applied by a debris flow against structures have been proposed [1–4]:

$$p_{\max} = \frac{\rho v^4}{gh}; \quad F = (5 \div 12)\rho h v^2 \qquad (1–2)$$

$$p_{\max} = (2 \div 5)\rho v^2; \quad F = \delta \cdot (\rho \cdot c \cdot v) \cdot h \qquad (3–4)$$

ρ being the flow density; v, the impact velocity; h, the flow depth; c, the fluid celerity; g, the acceleration gravity; δ, a numerical coefficient ranged between 0.75÷0.9 [4]. For the impact of mudflows against structures, the following relationship is proposed [5]:

$$p_{\max} = c_d \rho A \frac{v^2}{2} \qquad (5)$$

in which $A = bh$ represents the contact area; b, the flow width (for 2D cases, $b = 1$); c_d, the resistance coefficient evaluable as: $c_d = 0.18 \cdot F_r + 1.4$, with F_r, Froude number [5]. All previously described expressions show the dependence of the maximum pressure p_{max} or force F on the velocity (v) of the granular flow at the impact zone with rigid structures. A granular flow generally reaches the maximum velocity at the end of the '*first*' slope, where safeguarding measures (e.g. walls, barriers) are usually built. Thus, two analytical (*block*) models to estimate the maximum velocity reached by *coarse* and *fine* grained material flows are developed and proposed.

2 Main phenomena affecting coarse grained material flows

Experimental observations showed the growth of a basal "*shear layer*" [6], where initially large deformations and then dilation, *collisions* and *granular temperature* occur. By colliding each on others and with an irregular sliding surface, the particles change instantaneously their velocity (module and direction) and exhibit a sudden fluctuation (Fig. 1). To synthetically represent the grains' motion within the *shear layer*, the concept of *granular temperature* (T_g), defined as the average value of the square of the grains' velocity fluctuations with respect to their mean velocity, is introduced [7]. These velocity fluctuations nearly assume a Maxwellian distribution [8]; thus, T_g should be more properly defined by the variance of the velocity fluctuations [9]. For simplicity, T_g can be assumed proportional to the square of the shear rate [10]:

$$T_g = \frac{1}{15(1-e)}\left[1 + \frac{\pi}{12}\left(1 + \frac{5}{8 \cdot \nu_s g_0}\right)^2\right] \cdot \left(d_p \frac{dv}{dy}\right)^2 \qquad (6)$$

* Corresponding author: fdrfnc@gmail.com

e being the restitution coefficient (ϵ [0,1]; $e < 1$ must be considered due to the inelastic nature of the collisions); $v(y)$, the grain velocity profile (y, normal to the shear direction); d_p, the average grain diameter; ν_s , the solid fraction, which may assume the maximum value ν_{max} (equal to 0.74 for spherical grains); g_0, the radial distribution function: $g_0(\nu_s) = (1 - \nu_s/\nu_{max})^{-2.5\cdot\nu max}$ [11].

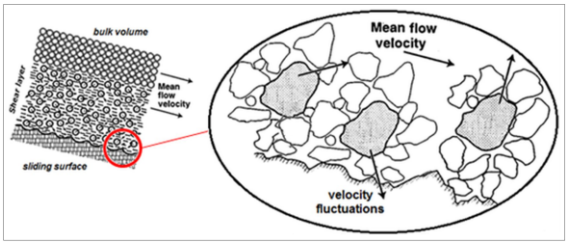

Fig. 1. Particles colliding with an irregular sliding surface, within the *shear layer*, inducing fluctuations of their velocity.

High speed relative motion and collisions between grains taking place within the *shear layer*, causing a *fluidification* effect [12] coupled with energy dissipations, require the development of complex resistance laws. The velocity field in coarse-grained material flows can be assumed to be composed of a *frictional* regime and a *collisional* regime [13]. In *frictional regime*, the shear stresses satisfy the Mohr-Coulomb resistance law: $\tau_{fr} = \sigma' \cdot \tan\varphi_b$, σ' being the effective normal stress; φ_b, the dynamic friction angle at the base of the granular mass. In *collisional regime*, the stress component normal to the boundary (*"dispersive pressure"*) and the shear stress component are expressed as follows [14]:

$$p_{disp} = a_i \rho_s \lambda^2 d_p^2 \cos\phi \left(\frac{\partial v}{\partial y}\right)^2 ; \tau_{disp} = a_i \rho_s \lambda^2 d_p^2 \sin\phi \left(\frac{\partial v}{\partial y}\right)^2 \quad (7\text{–}8)$$

a_i being the Bagnold coefficient (suggested value 0.042); ρ_s, the solid fraction mass density; λ, the linear concentration, that is a function of solid fraction ν_s ($\lambda = 1/[(\nu_{max}/\nu_s)^{1/3}-1]$); ϕ, the internal dynamic friction angle of granular bulk. Thus, the (total) shear stress τ_{max} is obtained by adding the frictional shear stress τ_{fr} to the dispersive shear stresses τ_{disp} . Resistance laws splitting these two contributions ($\tau_{max} = \tau_{fr} + \tau_{disp}$) have been therefore proposed [15, 16]; rheological models where both the *frictional* and *collisional* contributions are coupled into a single term, are also available [17].

Rapid change of pores volumes related to the continuous grains rearrangement [18] within the *shear layer* can generate excess pore water pressures at the base of coarse-grained material flows. Specific test show that the pore water pressure is maintained during the motion of sliding granular mass without dissipation [19]. Fragmentation (or grains' size reduction) can reduce the available energy and then mobility. The specific energy (kW·h/ton) required for grains' fragmentation is expressed as follows [20]:

$$W_{frag} = 10 \cdot W_{Bond} \left(d_{p,fin}^{-1/2} - d_{p,in}^{-1/2} \right) \geq 0 \quad (9)$$

only if $d_{p,fin} < d_{p,in}$. W_{Bond} is the Bond work index (kW·h/ton), depending on the type of granular material; $d_{p,in}$ and $d_{p,fin}$ are the size (in μm) of the grains before and after crushing, respectively; $d_{p,fin} = 1.04\cdot10^{-4}\cdot(W_{bond}/H_g)^2$, H_g being the geodetic difference in level; in this case W_{bond} is expressed in J/kg and $d_{p,fin}$ in cm.

3 Main phenomena affecting fine grained material flows

Fine - grained material flows are typically characterized by a high concentration of silts and clays. According to field observations and measurements [21], it is possible to state that the triggering mechanism and successive propagation mainly depend on excess pore water pressures followed by consolidation process. The excess pore water pressures can be generated by *(i)* shear strains induced by an earthquake; *(ii)* undrained loading following human activities; *(iii)* rapid accumulation of rainwater in soil layers with low permeability; *(iv)* seepage flow in boundary materials. The considerable shear strength reduction, following the generation of the excess pore water pressures, is often the main reason of high mobility of unstable fine-grained material volumes, even on very gentle slopes; furthermore, high pore water pressures can also induce the partial or complete liquefaction of the soil [19]. Conversely, the consolidation process of fine-grained materials [22-23], along the motion, progressively reduces the pore water pressure; the corresponding increase of the shear strength causes a reduction of the travelled distance.
For materials, characterized by $d_p < 0.02$ m, the energy dissipation due to grain collisions can be neglected [16].

4 Proposed models

Both proposed models are based on the following hypotheses (Fig. 2a): *(i)* the sliding granular mass is represented by a block (parallelepipedal shape) of thickness h, length l and width b (d_w is the depth, from the upper surface of the block, of the groundwater); *(ii)* the granular flow runs along planar surface of constant slope α_1 and length L (deformations induced by the possible variations of sliding surface are neglected [24]); *(iii)* although it is well-known that the mass of a debris flow may change due to erosion or deposition processes [12, 16], for the sake of simplicity, the debris flow mass is assumed constant.

4.1 Coarse-grained material flows modeling

An *energy-based* model is developed to describe the mobility of coarse-grained material flows [16], by taking into account the effects of *collisions* and *granular temperature*. The granular sliding body is composed of two layers (Fig. 2b) of equal basal area ($\Omega = l\cdot b$) and length l, representing the *shear layer* (thickness s^s) and the overlying mass (thickness s^b, "*block*") respectively. By imposing the equilibrium orthogonally to the sliding surfaces, the resulting force N_{tot} (= $W_b\cdot\cos\alpha_1$, W_b being

the weight of the block, Fig. 2b) must be balanced by the lithostatic (total) stresses, $\sigma = \rho^b g h \cdot \cos\alpha_1$ (ρ^b being the density of the block), coupled to the dispersive pressures, p_{disp} (eq. (7)):

$$W_b \cos\alpha_1 = \sigma \cdot \bar{r}(\dot{x})\Omega + p_{disp} \cdot r(\dot{x})\Omega \qquad (10)$$

r and $\hat{r}$ (=1 – r), dependent on the velocity ($v = \dot{x}$), have been suitably introduced to allow a *weighted* balance of the force N_{tot} according to the resulting lithostatic force and the resultant of the colliding forces statistically acting along the irregular sliding surface [16]:

$$r(v) = \frac{1}{\pi}\{\arctan[\eta(v - v_{cr})] - \arctan[-\eta(v + v_{cr})]\} \qquad (11)$$

η is a parameter falling in the range 0.005÷0.5, which modulates the shape of r; v_{cr} is the critical speed for which the regime dominated by the inertial forces becomes a *collisional* regime [16].

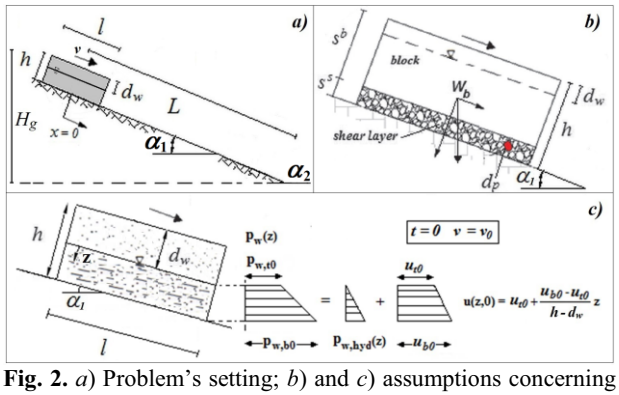

Fig. 2. *a*) Problem's setting; *b*) and *c*) assumptions concerning coarse and fine grained material flows modeling, respectively.

The eq. (10) allows to determine the thickness of the overlying block (if a linear change of velocity along y is assumed, the dispersive pressures p_{disp}, τ_{disp} and T_g become proportional to $\dot{x}^2$): $s^b(\dot{x}) = (1 - r) \cdot h + r \cdot Q_1 \lambda^2 \dot{x}^2$, where $Q_1 = a_i \rho^s d_p^2 \cdot \cos\phi / (\rho^b g \cdot \cos\alpha_1)$ and ρ^s is the density of *shear layer*. Because the sum of the masses of the *shear layer* (m^s) and the overlying block (m^b) equals the total sliding mass (m): $m = m^b + m^s = (\rho^b s^b + \rho^s s^s) \cdot \Omega$, the thickness of the shear layer s^s is thus expressed as: $s^s(\dot{x}) = (m - \rho^b s^b(\dot{x})\Omega)/(\rho^s \Omega)$. If a constant value is assigned to the interstitial pressure ($p_{w,b}$) at the base of the granular mass [18] and isopiezic lines are orthogonal to the motion direction: $p_{w,b} = p_{w,b,hyd} = \gamma_w (h - d_w) \cdot \cos\alpha_1$ (γ_w being the water unit weight; $d_w < 0$ allows to simulate the excess pore water pressure). The power balance of the sliding mass is expressed as [16]:

$$\dot{E}_p(t) + \dot{E}_k(t) + \dot{E}_r(t) + \dot{E}_{coll}(t) + \dot{E}_{gt}(t) + \dot{E}_{frag}(t) = 0 \qquad (12)$$

where $\dot{E}_p$ is the potential power ($=\dot{E}_p^{\,b} + \dot{E}_p^{\,s}$, $\dot{E}_p^{\,b}$ and $\dot{E}_p^{\,s}$ being the potential power of the block and *shear layer*, respectively); $\dot{E}_k$ is the kinetic power of the sliding mass ($=\dot{E}_k^{\,b} + \dot{E}_k^{\,s}$, $\dot{E}_k^{\,b}$ and $\dot{E}_k^{\,s}$ being the kinetic power of the block and *shear layer*, respectively); $\dot{E}_r$, is the power related to the energies dissipated along the sliding surface due to friction and dispersive pressures ($\dot{E}_r = T_{max} \cdot \dot{x}$, $T_{max} = T_{fr} + T_{disp}$; $T_{fr} = \tau_{fr} \cdot (1 - r) \cdot \Omega$, $T_{disp} = \tau_{disp} \cdot r \cdot \Omega$); $\dot{E}_{coll}$ is the power dissipated due to grain collisions; $\dot{E}_{gt}$ is the power stored as *granular temperature*; $\dot{E}_{frag}$ is the power lost by crashing or fragmentation [16].

4.2 Fine-grained material flows modeling

It is assumed a trapezoidal initial pore water pressure distribution ($p_w(z)$) within a basal saturated layer of thickness (h-d_w) (Fig. 2c); the initial values $p_{w,t0}$ and $p_{w,b0}$ of pore water pressure, at the top and the base of the saturated layer, depend on the values of hydrostatic interstitial pressure ($p_{w,hyd}(z) = \gamma_w z \cdot \cos\alpha_1$) and on the excess pore water pressure $u(z,t)$ (z, normal to the sliding surface, directed downward, from the upper surface of the saturated soil layer, Fig. 2c). Thus, the resultant U of the pore water pressures at the base of the sliding mass ($p_{w,b}(t)$), is equal to the sum of the basal hydrostatic interstitial pressure ($p_{w,b,hyd}$) and the basal excess pore water pressure at time t ($u(z=h-d_w,t) = u_b(t)$): $U = p_{w,b}(t) \cdot \Omega = (p_{w,b,hyd} + u_b(t)) \cdot \Omega$. If the involved material is not affected by dilatancy, the basal excess pore water pressures are dissipated during the motion due to consolidation process. Their evolution, referred to the case of impermeable horizontal base and drainage only through the upper surface of the saturated soil layer, is simply described through the following dissipation law $u_b(t)$ [25]: $u_b(t) = u_{b,0} \cdot e^{-at}$, where a is a parameter related to the variables that govern the consolidation process of the involved material ($a = \pi^2 c_v / (4 \cdot H^2)$, c_v being the 1-D consolidation coefficient; H, the drainage distance); u_{b0} is the initial basal excess pore water pressure, evaluable as: $u_{b0} = r_{0,b} \cdot u_{b,0,max}$, with $u_{b,0,max} = [(h - d_w)\gamma' + d_w \cdot \rho g] \cdot \cos\alpha_1$ (γ' is the submerged soil unit weight) and $r_{0,b} < 1$ to avoid the soil liquefaction. Under the previous assumptions, the motion's law is expressed as follows:

$$mg\sin\alpha_1 - \left[mg\cos\alpha_1 - \left(p_{w,b,hyd} + u_b(t)\right)\Omega\right]\tan\varphi_b = m\frac{dv}{dt} \qquad (13)$$

5 Comparison among measured data and theoretical results

Coarse-grained materials. The Acquabona Creek's debris flow, occurred in June 1997 in the Dolomites (Eastern Alps, Italy), was directly observed. Channel cross-section measurements taken along the flow channel indicate debris flow velocity ranging from 3.1 to 9.0 m/s [26]. After reworking the measured data, the following main parameters may be selected: L = 1250 m; $\alpha_1 = 18°$; l = 75 m; h = 2 m; Ω = 300 m^2; d_p = 0.03 m. The values of remaining parameters describing the mechanical behaviour, reported in Fig. 3, have been chosen according to previous parametrical analyses [16]. The proposed model allows to fit the measured maximum velocity, the speed evolution ($v(x)$) along the path and the observed maximum traveled distance. If the value of a single parameter (e.g. η) is changed, the fitting is not obtainable (curves *b*, *c*; Fig. 3).

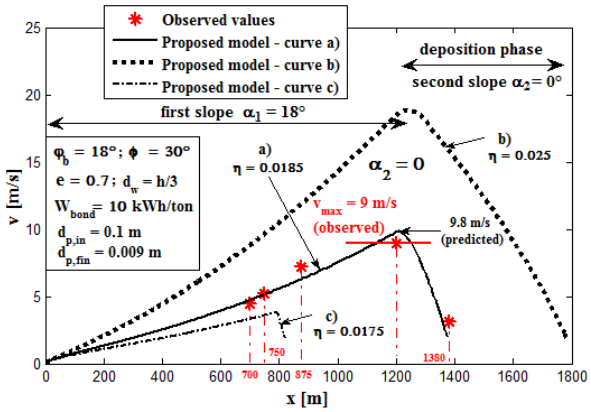

Fig. 3. Acquabona Creek's debris flow: measured and theoretical velocity (v) vs distance travel (x).

Fine-grained materials. Laboratory tests were performed with mixtures of water and sediment collected from the Rio Gadria material flow deposits (Eastern Alps, Italy) [27]. The involved material was characterized by an appreciable muddy component (d_p = 1 mm; ν_s = 0.55). The experimental apparatus is shown in Fig. 4: it is composed of flume of length 2 m, width 0.15 m, height 0.40 m, slope angle 20°. During the sliding of the material, the velocity was measured in four different cross sections (P_i, Fig. 4) of the flume. By assigning the following input parameters: L = 2 m; h = 0.20 m; l = b = 0.15 m; α_1 = 20° (the other parameters, reported in Fig. 4, have been determined according to parametrical analyses [22]), through the proposed model, the results shown in Fig. 4 are obtained.

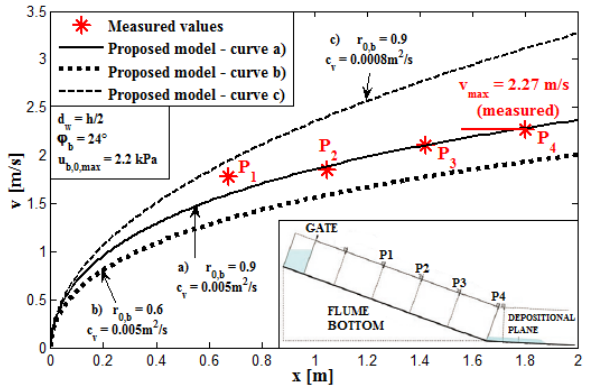

Fig. 4. Laboratory tests on fine-grained material flow: measured and theoretical velocity (v) vs distance travel (x).

Through the rational choice of input parameters, the proposed model allow to fit the measured values of velocity reached by material flow along its path. Again, the fitting is not obtainable by changing the selected parameters (e. g. c_v or $r_{0,b}$; curves b, c; Fig. 4).

6 Concluding remarks

Two analytical (block) models to estimate the velocity of *coarse* and *fine* – grained materials flows are proposed. The models are based on some simplified assumptions concerning the geometry of the granular mass (*block*) and sliding surface (*planar*), the evolution of pore water pressures (*1-D consolidation*), the energy dissipation (*friction, collisions, fragmentation*). Furthermore, they depend on some unconventional and empirical input parameters (e, η, v_{cr}, $r_{0,b}$), necessary to describe the physical and mechanical behaviour of *coarse* and *fine* – grained material flows. Their values may be obtained by the comparison between the measured and theoretical values of velocity.

References

1. Y. Fukui, M. Nakamura, H. Shiraishi, Y. Sasaki, Coastal Eng. Jpn., **6**, 67 – 82 (1963)
2. A. Daido, *XXV IAHR Congress, Technical Session B*. **3**, 211 – 213 (1993)
3. S. Zhang, Natural Hazards, **7**, 1 – 23 (1993)
4. F. Federico, A. Amoruso, IJEGE **1**, 5 – 24 (2008)
5. A. Armanini, C. Dalrì, F. Della Putta, M. Larcher, L. Rampanelli, M. Righetti, *Hydraulics of Dams Structures,* Taylor & Francis Group, London, ISBN 9058096327 (2004)
6. O. Hungr, Can. Geot. J., **32** (4), 610 – 623 (1995)
7. S. Ogawa, *US Japan Seminar on Continuum Mechanical and Statistical Approaches in the Mechanics of Granular Materials*, Tokyo (1978)
8. S. Warr, G.T.H. Jacques, J.M. Huntley, Powder Technology, **81**, 41 - 56 (1994)
9. D. Gollin, E. Bowman, P. Shepley, *6th Int. Symp. On Deformation Characteristics of Geomaterials*, Buenos Aires (2015)
10. A. Armanini, *XXXII Convegno Nazionale di Idraulica e costruzioni Idrauliche*, Palermo (2010)
11. S.B. Savage, C.K.K. Lun, J. of Fluid Mech., **189**, 311–335 (1988)
12. O. Hungr, S.G. Evans, *7th International Symposium on Landslides*, Trondheim, **11**, 233–238 (1996)
13. D. Zhang, M.A. Foda, Acta Mechanica, **136** (3), 155–170 (1999)
14. R.A. Bagnold, *R. Soc. London A*, **225**, 49–63 (1954)
15. A. Armanini, J. of Hydr. Res., **51**, 111–120 (2013)
16. F. Federico, C. Cesali, Can. Geot. J., **52**,1–21 (2015)
17. P. Jop, Y. Forterre, O. Pouliquen, Nature, 441, 727-730 (2006)
18. A. Musso, F. Federico, G. Troiano, Comp. and Geotech., **31**, 209–226 (2004)
19. R.M. Iverson, American Geophysical Union (1997)
20. F.V. De Blasio, Acta Mech., **221**, 375–382 (2011)
21. J.N. Hutchinson, R.K. Bhandari, Geotechnique, **21**, 353–358 (1971)
22. J.N. Hutchinson, Can. Geot. J., **23**, 115–126 (1986)
23. M. Pastor, J.A. Quecedo, F. Merodo, M.I. Herreros, E. González, P. Mira. Numerical modelling in Geomechanics, **6** (6), 1213-1232 (2002)
24. A. Taboada, K.J. Chang, *J. Geoph. Res*., **114** (2009)
25. J.A. Fernández-Merodo, G. Herrera, P. Mira, J. Mulas, M. Pastor, L. Noferini, D. Mecatti, G. Luzi, *Inter. Env. Model. and Soft. S.,* 1476-1483 (2008)
26. M. Berti, R. Genevois, A. Simoni, P.R. Tecca, Geomorphology, **29**, 265-274 (1999)
27. F. Bettella, G.B. Bischetti, V. D'Agostino, S.V. Marai, E. Ferrari, T. Michelini, J. of Agricultural Engineering, **46**, 4 (2015)